Journal of Molecular Structure 1019 (2012) 130–134

Contents lists available at SciVerse ScienceDirect

Journal of Molecular Structure

journal homepage: www.elsevier.com/locate/molstruc

# Molecular design of new hydrazone dyes for dye-sensitized solar cells: Synthesis, characterization and DFT study

Abdullah G. Al-Sehemi [a,*], Ahmad Irfan [a,*], Abdullah M. Asiri [b,c], Yousry Ahmed Ammar [a]

[a] Chemistry Department, Faculty of Science, King Khalid University, Abha, Saudi Arabia
[b] Chemistry Department, Faculty of Science, King Abdulaziz University, P.O. Box 80203, Jeddah 21589, Saudi Arabia
[c] Center of Excellence for Advanced Materials Research, King Abdulaziz University, P.O. Box 80203, Jeddah 21589, Saudi Arabia

ARTICLE INFO

*Article history:*
Received 11 January 2012
Accepted 15 February 2012
Available online 24 February 2012

*Keywords:*
Dye-sensitized solar cells
Density functional theory
Absorption
Transport properties

ABSTRACT

Three new sensitizers 2-{4-[2-(4-Nitrobenzylidene)hydrazino)]phenyl}ethylene-1,1,2-tricarbonitrile (**NBHPET**), 2-{4-[2-p-Chlorobenzylidenehydrazino]phenyl}- ethylene-1,1,2-tri carbonitrile **(CBHPET)** and 2-{4-[2-p-Bromobenzylidenehydrazino] phenyl}ethylene-1,1,2-tricarbonitrile **(BBHPET)** have been synthesized. The dyes showed pronounced solvatochromic effects as the polarity of the solvents increased. The structures have been optimized at B3LYP/6-31G(d) level of theory. The torsion in E-isomer is smaller than Z-isomer and azo isomers. The highest occupied molecular orbitals are delocalized on whole molecule while lowest unoccupied molecular orbitals are distributed on the tricarbonitrile. The lowest unoccupied molecular orbital energies are above the conduction band of titanium dioxide, highest occupied molecular orbitals of the dyes are below the redox couple of new synthesized dyes and small energy gap revealed these dyes would be better sensitizers for dye-sensitized solar cells.

## 1. Introduction

The first efficient dye-sensitized solar cells (DSSCs) were reported by O'Regan and Gratzel [1]. The DSSCs have attracted interest due to their moderately high power conversion efficiency and potentially low cost of production [2–5]. The most successful sensitizers employed in these cells are ruthenium polypyridyl complexes with power conversion efficiencies up to 11–12% [6]. However, Ru complexes contain a heavy metal, which is undesirable from environmental point of view [7]. Moreover, the process to synthesize the complexes is complicated and costly. In addition to Ru complexes, metal-free organic dyes as sensitizers are also under intensive investigation due to their high molar extinction coefficients, flexible structural modifications and low costs, and to date some of them have reached good efficiency [8–12].

The basic function is to prepare such dyes which are very much competent for DSSC, and which fulfill the basic requirements of design. Firstly, the sensitizing dyes must firmly stick to the photo catalyst plane to make sure very rapid electron insertion into the conduction band of $TiO_2$. Secondly, the lowest unoccupied molecular orbital (LUMO) of the dye must be adequately higher than the conduction band of $TiO_2$ for efficient charge insertion. The highest occupied molecular orbital (HOMO) of the dye must be lower than the hole-transport material (HTM) for efficient regeneration of the oxidized dye [13,14]. In recent years, DFT has been widely used to study the structures and absorption spectra of sensitizers for DSSCs [15].

Three new sensitizers 2-{4-[2-(4-Nitrobenzylidene)hydrazino)]-phenyl}ethylene 1,1,2-tricarbonitrile (**NBHPET**), 2-{4-[2-p-Chlorobenzylidenehydrazino]phenyl} ethylene-1,1,2-tri carbonitrile **(CBHPET)** and 2-{4-[2-p-Bromobenzylidenehydrazino] phenyl}ethylene-1,1,2-tricarbonitrile **(BBHPET)** have been synthesized, see Scheme 1. The effect on electronic properties, absorption and IR spectra has been investigated. By using density functional theory (DFT), we have shed light on the electronic and optical properties. We have also discussed the structure–property relationship. In addition, the prepared compounds were subjected to computational study to make a comparison between the experimental and theoretical data.

## 2. Experimental methods

Melting points were recorded on a Thomas-Hoover capillary melting apparatus without correction. IR spectra were taken as KBr disk on a Nicolet Magna 520 FTIR Spectrometer, $^1$H-NMR were recorded in DMSO-$d_6$ on a Bruker DPX 400 Spectrometer using TMS as internal standard. UV–vis spectra were recorded on a Shimadzu 260 Spectrometer for solutions.

---

* Corresponding authors. Tel.: +966 72418632; fax: +966 72418426.
*E-mail addresses:* agmasq@gmail.com (A.G. Al-Sehemi), irfaahmad@gmail.com (A. Irfan).

0022-2860/$ - see front matter © 2012 Elsevier B.V. All rights reserved.
doi:10.1016/j.molstruc.2012.02.035

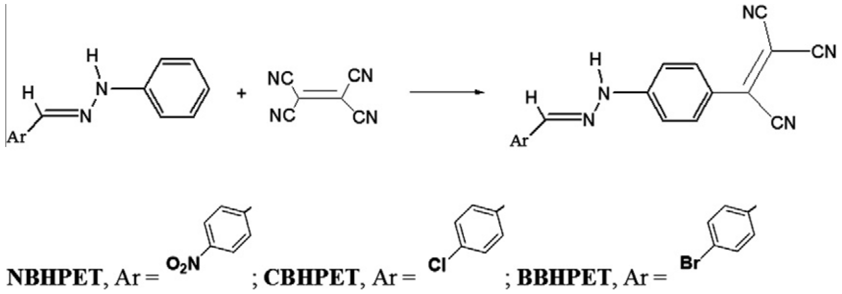

**Scheme 1.** The systematic sketch of new synthesized sensitizers **NBHPET**, **CBHPET**, **BBHPET**.

**Table 1**
Optimized geometrical parameters of investigated Systems at B3LYP/6-31G* level of theory.

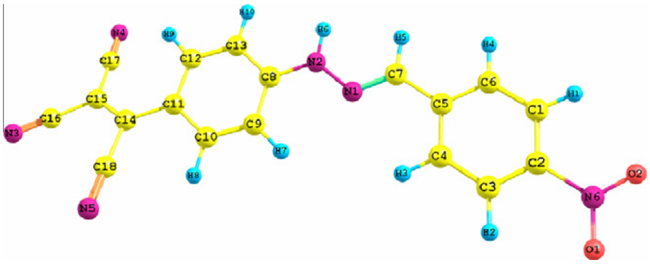

| Systems | Bond lengths (Å) | | | | | |
|---|---|---|---|---|---|---|
| | C5—C7 | C7—N1 | N1—N2 | N2—C8 | C8—C9 | C11—C14 |
| **NBHPET**-E | 1.459 | 1.289 | 1.345 | 1.379 | 1.407 | 1.460 |
| **NBHPET**-Z | 1.475 | 1.291 | 1.350 | 1.383 | 1.407 | 1.461 |
| **NBHPET**-azo | 1.515 | 1.474 | 1.249 | 1.431 | 1.403 | 1.473 |
| **CBHPET**-E | 1.459 | 1.288 | 1.351 | 1.375 | 1.409 | 1.458 |
| **CBHPET**-Z | 1.476 | 1.290 | 1.355 | 1.379 | 1.408 | 1.458 |
| **CBHPET**-azo | 1.508 | 1.481 | 1.248 | 1.431 | 1.403 | 1.472 |
| **BBHPET**-E | 1.459 | 1.288 | 1.351 | 1.375 | 1.409 | 1.458 |
| **BBHPET**-Z | 1.476 | 1.290 | 1.355 | 1.379 | 1.408 | 1.458 |
| **BBHPET**-azo | 1.508 | 1.481 | 1.248 | 1.431 | 1.403 | 1.472 |

| Systems | Dihedral angles (degrees) | | |
|---|---|---|---|
| | C5—C7—N1—N2 | C7—N1—N2—C8 | N1—N2—C8—C9 |
| **NBHPET**-E | 179.9 | 179.8 | −0.091 |
| **NBHPET**-Z | 2.254 | 176.8 | 8.240 |
| **NBHPET**-azo | 125.2 | −179.9 | 5.869 |
| **CBHPET**-E | 180.0 | 179.8 | −0.004 |
| **CBHPET**-Z | −2.189 | −177.2 | −8.684 |
| **CBHPET**-azo | 0.414 | −179.7 | 5.129 |
| **BBHPET**-E | −179.9 | 179.8 | 0.341 |
| **BBHPET**-Z | 2.193 | 177.0 | 8.847 |
| **BBHPET**-azo | 0.778 | −179.9 | 4.903 |

### *2.1. General procedure for the reaction of TCNE with hydrazones*

A solution of aromatic amine (10 mmol) and TCNE in DMF (25 ml) was stirred at 60–90 °C for 8 h. The solvent was removed and the residual solid was collected and recrystallized from toluene–chloroform mixture.

**NBHPET**) 2-{4-[2-(4-Nitrobenzylidene)hydrazino)]phenyl}ethylene-1,1,2-tricarbonitrile: [$C_{18}H_{10}N_6O_2$(342.31)], M. p. 265–267 °C, yield 70%; UV–vis (ethanol): $\lambda_{max}$ (nm) 519, 417, 262; IR $\upsilon$ ($cm^{-1}$): 3279 (sec. NH), 2217 (CN), 1614 (C=N), 1343 (C—N); $^1$HNMR (DMSO-$d_6$): 7.20–8.20 (m, 8H, Ar—H), 8.30(s, 1H, CH=N), 10.80(s, 1H, NH). $^{13}$C NMR (DMSO-$d_6$): 82.08, 147.33 (C=C), 3 × 113.38(3CN), 2 × 112.53, 2 × 124.0, 126.00, 2 × 127.55, 2 × 132.59, 137.95, 141.8, 150.64(12C—Ar), 162.28(CH=N).

**CBHPET**) 2-{4-[2-p-Chlorobenzylidenehydrazino]phenyl}ethylene-1,1,2-tri carbonitrile: [$C_{18}H_{10}ClN_5$(331.76)], m.p. > 300 °C. UV–vis (ethanol): $\lambda_{max}$ (nm) 530, 325; IR $\upsilon$ ($cm^{-1}$): 3263 (sec. NH), 2216 (CN), 1610 (C=N), 1337(C—N); $^1$HNMR (DMSO-$d_6$): 7.49–8.0 (m, 8H, Ar—H), 8.11 (s, 1H, CH=N), 11.88 (s, 1H, NH). $^{13}$C NMR (DMSO-$d_6$): 79.94, 142.92 (C=C), 3 × 114.7 (3CN), 112.96, 2 × 113.76, 119.27, 128.42, 2 × 128.82, 2 × 132.63, 133.18, 134.13, 137.33, (12C—Ar) 151.03 (CH=N).

**BBHPET**) 2-{4-[2-p-Bromobenzylidenehydrazino]phenyl}ethylene-1,1,2-tricarbonitrile: [$C_{18}H_{10}BrN_5$(376.21)], m.p. > 300 °C. UV–vis (ethanol): $\lambda_{max}$ (nm) 530, 326; IR $\upsilon$ ($cm^{-1}$): 3267 (sec. NH), 2216 (CN), 1665 (C=N), 1336 (C—N); $^1$HNMR (DMSO-$d_6$): 7.63–7.99 (m, 8H, Ar—H), 8.08 (s, 1H, CH=N), 11.87 (s, 1H, NH). $^{13}$C NMR (DMSO-$d_6$): 79.97, 142.99 (C=C), 3 × 114.01 (3CN), 112.94, 2 × 113.76, 119.49, 122.91, 2 × 128.64, 2 × 131.72, 132.62, 137.32, 150.99, (12C—Ar) 162.22 (CH=N).

## 3. Computational methods

The structures of the investigated dyes have been optimized by using density functional theory (DFT) at the B3LYP/6-31G(d) level of theory [16–20]. The time dependant density functional theory (TD-DFT) has been applied to calculate the absorption spectra at the TD-B3LYP/6-31G(d) level of theory which has been previously used to predict good results [21,22]. The B3LYP/6-31G(d) level of theory ha been also adopted to calculate the thermodynamic parameters, i.e., relative energies ($\Delta E_0$), enthalpies ($\Delta H$) and free energies ($\Delta G$) (kcal/mol) for E, Z and azo isomers. All the calculations were carried out by using Gaussian03 program package [23]. Three possible classes of isomeric molecules for dyes are E, Z and azo isomerism are shown in Fig. S1. These isomers arise by rotating around torsion angles N1—N2—C5—C7 for investigated dyes. Then by fully optimization stable conformers have been achieved.

## 4. Results and discussion

### *4.1. Geometries*

The fully optimized structures of E, Z and azo isomers are shown in Fig. S1. The computed geometrical parameters of **NBHPET**, **CBHPET**, and **BBHPET** have been tabulated in Table 1. The C—C, C—N, and N—N bond lengths of E and Z isomers of **NBHPET**, **CBHPET**, and **BBHPET** are approximately similar except the C5—C7. The C5—C7 in Z isomer of **NBHPET**, **CBHPET**, and **BBHPET** stretch 0.016 Å and 0.017 Å compared to E isomer, respectively. We have observed that there is no significant change in bond lengths of azo isomers in **NBHPET**, **CBHPET**, and **BBHPET**. By comparing the bond lengths of the E, Z and azo isomer of **NBHPET**, we have observed that C5—C7 of azo isomer stretched 0.056 and 0.040 Å compared to E and Z isomer, respectively. The C7—N1 of azo isomer elongated almost 0.184 Å than E and Z isomers. The N1—N2 of azo isomer shortened 0.096 and 0.101 Å while N2—C8

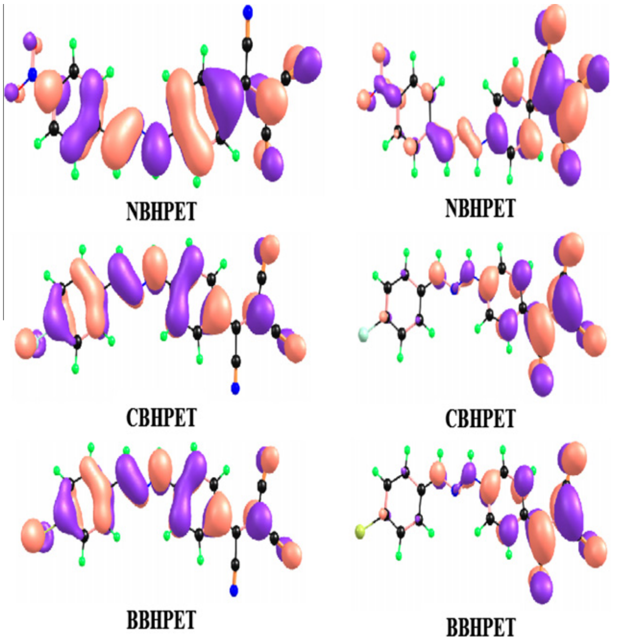

**Fig. 1.** The HOMOs (left) and LUMOs (right) of the most stable isomers of investigated dyes.

**Table 2**
HOMO energy ($E_{HOMO}$), LUMO energy ($E_{LUMO}$), HOMO–LUMO energy gap ($E_{gap}$) and absorption spectra ($\lambda_{max}$) in different solvents in eV.

| Dyes | $E_{HOMO}$ | $E_{LUMO}$ | $E_{gap}$ | $E_{gap}$ | | | | |
|---|---|---|---|---|---|---|---|---|
| | | | | a | b | c | d | e |
| **NBHPET** | −6.42 | −3.61 | 2.81 | 512 | 519 | 509 | 533 | 528 |
| | | | | 400 | 417 | 393 | 427 | 415 |
| | | | | 263 | 262 | 262 | 252 | 290 |
| **CBHPET** | −6.11 | −3.39 | 2.72 | 523 | 530 | 520 | 573 | 537 |
| | | | | 321 | 325 | 324 | 238 | 367 |
| | | | | | | | | 321 |
| **BBHPET** | −6.10 | −3.39 | 2.71 | 522 | 530 | 521 | 563 | 539 |
| | | | | 322 | 326 | 324 | 254 | 375 |
| | | | | | | | | 322 |

[a]$CH_3CN$, [b]$CH_3CH_2OH$, [c]CHCl3, [d]DMSO, [e]TD-B3LYP/6-31G* in $CH_3CN$.

of azo isomer lengthened 0.052 and 0.048 Å than E and Z isomers, respectively. By substituting the chloro or bromo in place of nitro, we have observed no significant effect in lengthening or shortening of different bond lengths of the azo isomers. The torsion in E isomer is smaller than Z and azo isomers of **NBHPET**, **CBHPET**, and **BBHPET**.

### 4.2. Electronic properties and absorption spectra

The distribution pattern of the HOMOs and LUMOs has been shown in Fig. 1. We have observed that HOMOs are delocalized on entire molecule. The CN, Cl and Br of **NBHPET**, **CBHPET**, and **BBHPET** also take part in the formation of HOMOs, respectively. In **NBHPET** the LUMO is localized on whole molecule while in **CBHPET** and **BBHPET** the LUMOs are distributed on the tricarbonitrile. It is might be due that strong electron withdrawing group CN attract the charge density toward itself which leads to distribution of LUMO in **NBHPET** on whole dye. While Cl and Br are weak withdrawing groups compared to CN escort LUMOs on the tricarbonitrile. The HOMO–LUMO energy gap of these dyes was calculated at the B3LYP/6-31G(d) level of theory. The HOMO energy ($E_{HOMO}$), LUMO energy ($E_{LUMO}$) and HOMO–LUMO energy gap ($E_{gap}$) of **NBHPET**, **CBHPET**, and **BBHPET** has been tabulated in Table 2.

For good DSSC sensitizers following factors to be considered: a narrow band gap, with LUMO lying just above the conduction band of $TiO_2$ and HOMO below the redox couple. As a model for nanocrystallinity the HOMO and LUMO energies of bare cluster $(TiO_2)_{38}$ are −7.23 and −4.1 eV, respectively, resulting in a $E_{gap}$ of 3.13 eV [24]. Usually an energy gap more than 0.2 eV between the LUMO of the dye and the conduction band of the $TiO_2$ is necessary for effective electron injection [13]. The LUMO energies of studied dyes are above the conduction band of $TiO_2$. The HOMO of the redox couple ($I - /I_3^-$) is −4.8 eV [14]. It can be found that HOMOs of the dyes are below the redox couple. The smaller HOMO–LUMO energy gaps of **NBHPET**, **CBHPET**, and **BBHPET** revealed that these dyes would be efficient for DSSC.

The **NBHPET** showed absorption band at 509 nm in chloroform, 512 nm in $CH_3CN$ and 519 nm in ethanol. No significant effect has been observed in absorption spectra toward red shift by changing the solvent from chloroform to ethanol. Most significant effect toward bathochromic shift has been observed in DMSO (24 nm). In **CBHPET** and **BBHPET** the noteworthy red shifts 53 nm and 42 nm have been observed in DMSO compared to chloroform, respectively. It has been examined that **CBHPET** and **BBHPET** conferred red shift in different solvents compared to **NBHPET**. The dyes were measured in various solvents having different polarity.

The dyes were measured in various solvents having different polarity, see Table 2. The trend of absorption spectra toward red shift in different solvents is CHCl3 < $CH_3CN$ < $CH_3CH_2OH$ < DMSO. The absorption spectra of **CBHPET** and **BBHPET** in all the investigated sensitizers are almost same while absorption spectra of **NBHPET** are blue shifted. The maximum absorption spectra computed at TD-B3LYP/6-31G* level of theory is 528, 537 and 539 nm for **NBHPET**, **CBHPET** and **BBHPET**, respectively which are in good agreement with the experimental evidence, see Table 2.

### 4.3. IR spectra

The IR spectra of these new dyes exhibited three important absorption bands; the first band centered at 3279 $cm^{-1}$, 3563 $cm^{-1}$, and 3267 $cm^{-1}$ for the υNH absorption in **NBHPET**, **CBHPET**, and **BBHPET**, respectively. The second band is a sharp absorption band in the region of 2217 $cm^{-1}$ and 2216 $cm^{-1}$, which was attributed to the cyano group absorption in **NBHPET**, **CBHPET**, and **BBHPET**, respectively. The third is an absorption band in the region of 1614 $cm^{-1}$, 1610 $cm^{-1}$ and 1599 $cm^{-1}$ ascribed for the C=N absorption in **NBHPET**, **CBHPET**, and **BBHPET**, respectively, see Fig. 2. The tricyanovinylation undoubtedly takes place at a position para to the hydrazine group as evidenced from the $^1H$ NMR signals for doublet two hydrogen. The azomethine hydrogen of the synthesized dyes was located in the region of 8.1–9.13 ppm (see Supporting information for detail).

### 4.4. Thermodynamic stabilities

Thermodynamic parameters of isomers (E, Z and azo); relative energies, relative enthalpies and free energies for **NBHPET**, **CBHPET**, and **BBHPET** dyes have been tabulated in Table 3. The relative energy, $\Delta E_0$, is defined as a difference between its zero-point corrected total energy and that of the most stable one E, in each case. Relative enthalpies and free energies at 298 K are also defined as the difference between the enthalpy or free energy of a given E/Z or azo isomers and that of E form. As shown in Table 3, the order of relative stability of those isomers is the same when considering relative energy or relative free energy. DFT calculation shows that E isomers are the most stable.

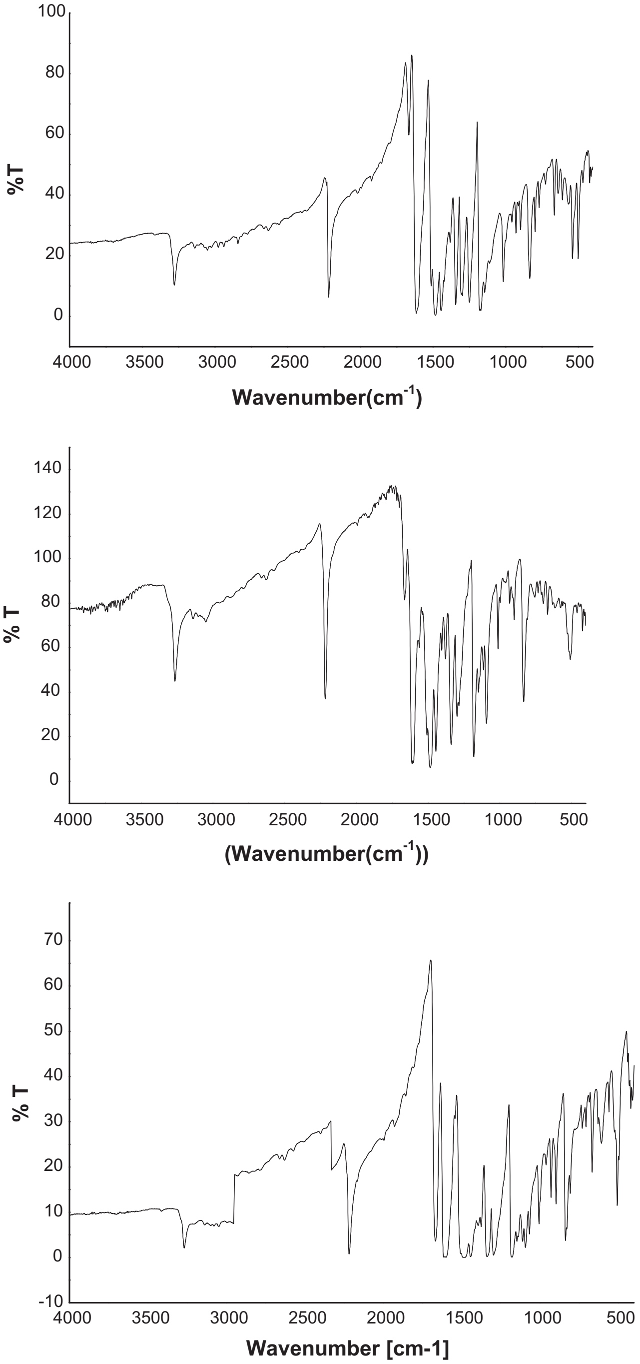

**Fig. 2.** IR spectra of **NBHPET** (top), **CBHPET** (middle) and **BBHPET** (bottom).

**Table 3**
Thermodynamic parameters (kcal/mol) for E, Z and azo isomers of studied Systems at B3LYP/6-31G(d) level.

| Systems | $\Delta E_0$ | $\Delta H$ | $\Delta G$ | $\Delta E$ | *Dipole* |
|---|---|---|---|---|---|
| **NBHPET**E | 0.00 | 0.00 | 0.00 | 0.00 | 7.9938 |
| **NBHPET** Z | 5.52 | 5.44 | 5.51 | 5.23 | 8.0644 |
| **NBHPET** azo | 14.7 | 14.8 | 13.6 | 15.2 | 5.328 |
| **CBHPET** E | 0.00 | 0.00 | 0.00 | 0.00 | 10.4355 |
| **CBHPET** Z | 4.87 | 4.78 | 4.97 | 4.55 | 10.9111 |
| **CBHPET** azo | 16.2 | 16.3 | 15.2 | 16.8 | 6.3133 |
| **BBHPET** E | 0.00 | 0.00 | 0.00 | 0.00 | 10.516 |
| **BBHPET** Z | 4.87 | 4.79 | 4.77 | 4.57 | 11.0582 |
| **BBHPET** azo | 16.2 | 16.3 | 15.4 | 16.8 | 6.3262 |

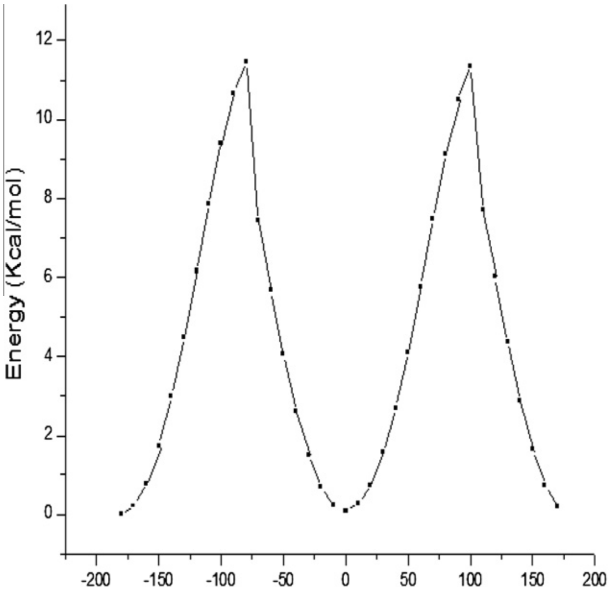

**Fig. 3.** Molecular energy profile using DFT against the selected torsional degree of freedom of **NBHPET**.

### 4.5. Conformation analysis

The initial guess for scanning calculation of the stable isomer E of **NBHPET** was first obtained from the optimization using B3LYP/6-31G(d) and transformed into the *Z*-matrix format with Babel program [25]. The starting geometry of E-isomers was obtained by dynamic procedure in HyperChem [26]. To identify low energy conformations, the potential energy surface shape has been examined at the B3LYP/6-31G(d) level. The potential energy surfaces of dihedral angle (N1—N2—C8—C9) from +180° to −180° in 5° or 10° steps (Fig. 2). The conformational energy profile shows two maxima near (−90 and 90°). The aromatic rings are nearly perpendicular at these values of selected torsion angle. The energy barriers may be due to the steric interactions between the π electrons of the two aromatic rings. It is clear from Fig. 3, there are three local minima observed at (−180, 0 and 180) for N1—N2—C8—C9 torsional angle and these are most stable conformers for this torsion angle. The DFT optimized geometry of these dyes is coplanar at these values of selected torsion angle.

## 5. Conclusions

By increasing the solvent polarity, bathochromic shift in absorption spectra has been observed. IR spectra of these new synthesized dyes exhibited three important absorption bands; the first band centered for the υNH absorption, second band is a sharp absorption band for cyano group absorption while third absorption band ascribed for the C=N absorption. The structures have been optimized at B3LYP/6-31G(d) level of theory. The chloro or bromo substitution in place of nitro has no significant effect in lengthening or shortening of different bond lengths of the azo isomers. The torsion in E isomer is smaller than Z and azo isomers of **NBHPET**, **CBHPET**, and **BBHPET**. DFT calculation shows that E isomers are the most stable. In **CBHPET** and **BBHPET**, the HOMOs are delocalized on entire molecule while LUMOs are distributed on tricarbonitrile. The LUMO energies of **NBHPET**, **CBHPET**, and **BBHPET** are above the conduction band of $TiO_2$. The HOMOs of the dyes are below the redox couple and smaller HOMO–LUMO energy gaps revealed that these dyes would be efficient for DSSC.

## Acknowledgment

The present work has been carried out under Project No. 08-NAN155-7 funded by KAUST (King Abdul Aziz City for Science and Technology) through the Long Term Comprehensive National Plan for Science, Technology and Innovation program.

## Appendix A. Supplementary material

Supplementary data associated with this article can be found, in the online version, at doi:10.1016/j.molstruc.2012.02.035.

## References

[1] B. O'Regan, M. Gratzel, Nature 353 (1991) 737–739.
[2] X. Liu, Y. Luo, H. Li, Y. Fan, Z. Yu, Y. Lin, L. Chen, Q. Meng, Room temperature fabrication of porous ZnO photoelectrodes for flexible dye-sensitized solar cells, Chem. Commun. (2007) 2847–2849.
[3] K.R.J. Thomas, Y.-C. Hsu, J.T. Lin, K.-M. Lee, K.-C. Ho, C.-H. Lai, Y.-M. Cheng, P.-T. Chou, Chem. Mater. 20 (2008) 1830–1840.
[4] K. Hara, T. Sato, R. Katoh, A. Furube, T. Yoshihara, M. Murai, M. Kurashige, S. Ito, A. Shinpo, S. Suga, H. Arakawa, Adv. Func. Mater. 15 (2005) 246–252.
[5] R. Chen, X. Yang, H. Tian, L. Sun, J. Photochem. Photobiology A: Chem. 189 (2007) 295–300.
[6] C.-Y. Chen, M. Wang, J.-Y. Li, N. Pootrakulchote, L. Alibabaei, ACS Nano 3 (2009) 3103–3109.
[7] Y. Amao, T. Komori, Biosens. Bioelectron. 19 (2004) 843–847.
[8] T. Horiuchi, H. Miura, K. Sumioka, S. Uchida, J. Am. Chem. Soc. 126 (2004) 12218–12219.
[9] T. Horiuchi, H. Miura, S. Uchida, J. Photochem. Photobiol. A: Chem. 164 (2004) 29–32.
[10] T. Kitamura, M. Ikeda, K. Shigaki, T. Inoue, N.A. Anderson, X. Ai, T. Lian, S. Yanagida, Phenyl-conjugated oligoene sensitizers for $TiO_2$ solar cells, Chem. Mater. 16 (2004) 1806–1812.
[11] D.P. Hagberg, J.-H. Yum, H. Lee, F.D. Angelis, T. Marinado, K.M. Karlsson, R. Humphry-Baker, L. Sun, A. Hagfeldt, M. Grätzel, M.K. Nazeeruddin, J. Am. Chem. Soc. 130 (2008) 6259–6266.
[12] A. Mishra, M.K.R. Fischer, P. Bäuerle, Angew. Chem. Int. Ed. 48 (2009) 2474–2499.
[13] F.D. Angelis, S. Fntacci, A. Selloni, Nanotechnology 19 (2008) 424002–424008.
[14] S. Ito, S.M. Zakeeruddin, R. Humphry-Baker, P. Liska, R. Charvet, P. Comte, M.K. Nazeeruddin, P. Péchy, M. Takata, H. Miura, S. Uchida, Adv. Mater. 18 (2006) 1202–1205.
[15] M.K. Nazeeruddin, F.D. Angelis, S. Fantacci, A. Selloni, G. Viscardi, P. Liska, S. Ito, B. Takeru, M. Grätzel, J. Am. Chem. Soc. 127 (2005) 16835–16847.
[16] A.D. Becke, J. Chem. Phys. 98 (1993) 5648–5652.
[17] C. Lee, W. Yang, R.G. Parr, Phys. Rev. B 37 (1988) 785–789.
[18] P.J. Stephens, F.J. Devlin, C.F. Chabalowski, M.J. Frisch, J. Phys. Chem. 98 (1994) 11623–11627.
[19] B.J. Lynch, P.L. Fast, M. Harris, D.G. Truhlar, J. Phys. Chem. A 104 (2000) 4811–4815.
[20] J.P. Perdew, J.A. Chevary, S.H. Vosko, K.A. Jackson, M.R. Pederson, D.J. Singh, C. Fiolhais, Phys. Rev. B 46 (1992) 6671–6687.
[21] P.J. Walsh, K.C. Gordon, D.L. Officer, W.M. Campbell, J. Mol. Struct. – Thechem. 759 (2006) 17–24.
[22] D.M. Cleland, K.C. Gordon, D.L. Officer, P. Wagner, P.J. Walsh, Spectrochimica Acta Part A 74 (2009) 931–935.
[23] M.J. Frisch et al., Gaussian 03, revision C.02, Gaussian, Inc., Pittsburgh Wallingford, CT, 2004.
[24] M.P. Balanay, D.H. Kim, Phys. Chem. Chem. Phys. 10 (2008) 5121–5127.
[25] P. Walters, M. Stahl, Babel, version 1.1. Department of Chemistry, University of Arizona, Tucson, AZ 85721, 1994.
[26] HyperChem 7.5, Molecular Modeling System, HyperCube, Inc., Waterloo, Oterio, 2002.